Rapid uniform rotation of protoneutron stars

J.O. Goussard[2], P. Haensel[1,2], and J.L. Zdunik[1]

[1] N. Copernicus Astronomical Center, Polish Academy of Sciences, Bartycka 18, PL-00716 Warszawa, Poland
[2] Département d'Astrophysique Relativiste et de Cosmologie, UPR 176 du CNRS, Observatoire de Paris, Section de Meudon, F-92195 Meudon Cedex, France (goussard@obspm.fr, haensel@camk.edu.pl, jlz@camk.edu.pl)

Abstract. Rapid uniform rotation of newborn neutron stars (protoneutron stars) is studied for a range of internal temperatures and entropies per baryon predicted by the existing numerical simulations. Calculations are performed using general relativistic equations of hydrostatic equilibrium of rotating, axially symmetric stars. Stability of rotating configurations with respect to mass shedding and the axially symmetric perturbations is studied. Numerical calculations are performed for a realistic dense matter equation of state, under various assumptions concerning neutron star interior (large trapped lepton number, no trapped lepton number, isentropic, isothermal). For configurations with baryon mass well below the maximum one for the non-rotating models, the mass shedding limit depends quite sensitively on the position of the "neutrinosphere" (which has a deformed, spheroidal shape); this dependence weakens with increasing baryon mass. The absolute upper limit on rotation frequency is, to a good approximation, obtained for the maximum baryon mass of rotating configurations. Empirical formula for the maximum rotation frequency of uniformly rotating protoneutron stars is shown to be quite precise; it actually coincides with that used for cold neutron stars. Evolutionary sequences at fixed baryon mass and angular momentum, which correspond to evolution of protoneutron stars into cold neutron stars are studied, and resulting constraints on the maximum rotation frequency of solitary pulsars are discussed.

Key words: dense matter – stars: neutron – stars: pulsars

1. Introduction

Neutrons stars are born in gravitational collapse of massive, degenerate stellar cores. Newly born neutron stars are hot and lepton rich objects, quite different from ordinary low temperature, lepton poor neutron stars. In view of these differences, newly born neutron stars are called *protoneutron* stars; they transform

Send offprint requests to: J.O. Goussard

into standard neutron stars on a timescale of the order of ten seconds, needed for the loss of a significant lepton number excess via emission of neutrinos trapped in the dense, hot interior.

In view of the fact that the typical evolution timescale of a protoneutron star (seconds) is some three orders of magnitude longer, than the dynamical timescale for this objects (milliseconds), one can study its evolution in the quasistatic approximation (Burrows & Lattimer 1986). Properties of static (nonrotating) protoneutron stars, under various assumptions concerning composition and equation of state (EOS) of hot, dense stellar interior were studied by numerous authors (Burrows & Lattimer 1986, Takatsuka 1995, Bombaci et al. 1995, Bombaci 1996, Bombaci et al. 1996).

The scenario of transformation of a protoneutron star into a neutron star could be strongly influenced by a phase transition in the central region of the star. Brown and Bethe (1994) suggested a phase transition implied by the K^- condensation at supranuclear densities. Such a K^- condensation could dramatically soften the equation of state of dense matter, leading to a low maximum allowable mass of neutron stars. In such a case, the massive protoneutron stars could be stabilized by the effects of high temperature and of the presence of trapped neutrinos, and this would lead to maximum baryon mass of protoneutron star larger by some 0.2 $M_\odot$ than that of cold neutron stars. The deleptonization and cooling of protoneutron stars of baryon mass exceeding the maximum allowable baryon mass for neutron stars, would then inevitably lead to their collapse into black holes. The dynamics of such a process was recently studied by Baumgarte et al. (1996). It should be mentioned, however, that the very possibility of existence of the kaon condensate (or other exotic phases of matter, such as the pion condensate, or the quark matter) at neutron star densities is far from being established. Recently, for instance, Pandharipande et al. (1995) pointed out that kaon-nucleon and nucleon-nucleon correlations in dense matter raise significantly the threshold density for kaon condensation, possibly to the densities higher than those characteristic of stable neutron stars. In view of these uncertainties, we will restrict in the present paper to a standard model of dense matter, composed of nucleons and leptons.

The calculations of the static models of protoneutron stars should be considered as a first step in the studies of these objects. It is clear, in view of the dynamical scenario of their formation, that protoneutron stars are far from being static. Due to the nonzero initial angular momentum of the collapsing core, protoneutron stars are expected to rotate. On the other hand, the formation scenario involves compression (with overshoot of central density) and a hydrodynamical bounce, so that a newborn protoneutron star begins its life in a highly excited state, pulsating around its quasistatic equilibrium. In the present paper we study the rotation of protoneutron stars; pulsations of protoneutron stars will be discussed in a separate paper (Gondek, Haensel & Zdunik, in preparation).

Some aspects of rapid uniform rotation of protoneutron stars have been recently studied in (Takatsuka 1995, Hashimoto et al. 1995). However, the calculations reported by Takatsuka (1995) were actually done for static (non-rotating) protoneutron stars, and were then used to estimate the maximum rotation frequency of uniformly rotating protoneutron stars, Ω_{max}, via an "empirical formula". It should be stressed, that the validity of such an "empirical formula", which expresses Ω_{max} in terms of the mass and radius of the extremal *static* configuration with maximum allowable mass, had been checked only in the restricted case of *cold* neutron stars (Haensel & Zdunik 1989, Friedman et al. 1989, Shapiro et al. 1989, Haensel et al. 1995, Nozawa et al. 1996). Only isentropic equations of state were considered by Takatsuka (1995). Hashimoto et al. (1995) calculated the structure of stationary configurations of uniformly rotating protoneutron stars, using a two-dimensional general relativistic code. These authors restricted themselves to the case with zero trapped lepton number. They assumed a constant temperature in the hot interior of the star, and used a zero temperature (cold) EOS for $\rho < 10^{10}$ g cm^{-3}. It should be stressed, that the assumption of $T = const.$ corresponds to an isothermal state in the Newtonian (flat space-time) theory of gravitation. In general relativity, we will define isothermal state by $T^* = \frac{N}{\Gamma}T = const.$ (where N is the lapse function and Γ is the Lorentz factor, see Sect. 3.1), and the effects of the space-time curvature will turn out to be rather important for massive neutron stars. Also, their choice for the low density edge of the hot interior can be questioned. Finally, their criterion for finding maximally rotating configuration is actually valid only for cold ($T = 0$) or isentropic protoneutron stars: its use in the case of the $T = const.$ hot interior is unjustified (see Sect. 3.2 for a correct statement of the stability criterion). In a recent paper, Lai and Shapiro (1995) have studied the secular evolution, secular "bar instability", and the gravitational wave emission from the newly formed, rapidly rotating neutron stars. However, these authors used unrealistic (polytropic) equations of state of neutron star matter. Moreover, the calculations were done within Newtonian theory of gravitation. In view of this, the internal structure of their models of newly born neutron stars was quite different from that characteristic of the realistic models of protoneutron stars. The problem of the secular "bar instability" in rapidly rotating neutron stars was also studied, using general relativity, by Bonazzola et al

(1995). However, numerical calculations were done only for realistic equations of state of *cold* neutron star matter.

In the present paper we study the properties of uniformly rotating protoneutron stars, using exact relativistic description of the rapid, stationary rotation, combined with realistic equations of state of hot dense matter, used in the whole range of temperatures and densities relevant for protoneutron stars. In particular, we calculate the maximum frequency of uniform rotation of protoneutron stars and its dependence on their baryon mass, and on the thermal state and composition of stellar interior. It is clear, that uniform rotation represents only an approximation to the actual rotational state of a newly born protoneutron star. Existing numerical simulations of gravitational collapse of rotating cores of massive stars produce differentially rotating protoneutron stars (Janka & Moenchmeyer 1989a, b, Moenchmeyer & Mueller 1989). However, it should be stressed that the initial rotational state of collapsing core is unknown, and this implies uncertainty concerning the rotational state of resulting protoneutron star. It is reasonable to say, that the actual degree of nonuniformity of rotation of a protoneutron star should be considered as unknown. In the present paper we will not address the question of the physical mechanisms that could "rigidify" the rotational motion within the protoneutron star interior. However, we will use the approximation of uniform rotation in order to limit the number the parameter space for our numerical calculation, and also because of the relative simplicity of the stability analysis in this specific, idealized case.

Within our simplified model, the "neutrinosphere" (which has actually a deformed, spheroidal shape) will separate hot, neutrino-opaque interior of a protoneutron star (hereafter referred to as "hot interior") from a significantly cooler, neutrino-transparent envelope. The actual thermal state of the hot interior of protoneutron star is determined by its formation scenario, and is expected to be influenced by the dissipative processes (damping of pulsations, viscous damping of differential rotation, neutrino diffusion). For simplicity, we will restrict ourselves to two limiting cases: an isothermal ($T^* = \frac{N}{\Gamma}T = const.$, see Sect. 3), and an isentropic (entropy per baryon $s = const.$) hot interior. We will also consider two limiting cases of the lepton composition of the protoneutron star interior. The first case, referring to the very initial state of protoneutron star, will correspond to a fixed trapped lepton number. In the second case, neutrinos will not contribute to the lepton number of the matter, which will correspond to vanishing chemical potential of the electron neutrinos; such a situation will take place after a deleptonization of a protononeutron star. The position of the neutrinosphere will be located using a simple prescription based on specific properties of the neutrino opacity of hot dense matter. In all cases, the equation of state of hot dense matter will be determined using one of the models of Lattimer and Swesty (1991).

The plan of the paper is as follows. In Sect. 2 we describe the physical state of the interior of protoneutron star, with particular emphasis on the EOS of the hot interior at various stages of evolution. We explain also our prescription for locating the "neutrinosphere" of a protoneutron star, and we give some details concerning the assumed temperature profile within a protoneu-

tron star. Using simple estimates of the timescales relevant for various transport processes, we justify the approximation of stationarity which is used throughout this paper. In Sect. 3 we give a brief description of the exact equations, used for the calculation of stationary configuration of uniformly rotating protoneutron stars. We discuss also stability of rotating configurations with respect to the axially-symmetric perturbations. The numerical method, used for the calculation of rapidly rotating configurations of protoneutron star, is briefly described in Sect. 4, where we also discuss numerical precision of our solutions. Maximum rotation frequency, for various physical conditions prevailing in the hot stellar interior, calculated as a function of the baryon (rest) mass of protoneutron star, is presented in Sect. 5. Then, in Sect. 6 we show the validity of an empirical formula, which enables one to express with a surprisingly high precision the maximum frequency of rotating protoneutron stars in terms of the mass and radius of the maximum mass configuration of static (non-rotating) protoneutron stars with same EOS. In Sect. 7 we study the evolutionary transformation of a rotating protoneutron star into a cold neutron star. We show that, at fixed rest mass and angular momentum, maximum rotation frequency of protoneutron stars imposes severe constraints on the rotation frequency of solitary neutron stars. Finally, Sect. 8 contains discussion of our results and conclusion.

2. Physical state of the interior of protoneutron stars

We consider a protoneutron star (PNS) just after its formation. We assume it has a well defined "neutrinosphere", which separates a hot, neutrino-opaque interior from colder, neutrino-transparent outer envelope. Important parameters, which determine the local state of the matter in the hot interior are: baryon (nucleon) number density n, net electron fraction $Y_e = (n_{e^-} - n_{e^+})/n$, and the net electron-neutrino fraction $Y_\nu = Y_{\nu_e} - Y_{\bar{\nu}_e}$. The calculation of the composition of hot matter and of its EOS is described below.

2.1. Neutrino opaque core with trapped lepton number

Such a situation is characteristic of the very initial stage of existence of a PNS. Matter is composed of nucleons (both free and bound in nuclei) and leptons (electrons and neutrinos; for simplicity, we do not include muons). All constituents of the matter (plus photons) are in thermodynamic equilibrium at given values of n, T and $Y_l = Y_e + Y_\nu$. The composition of the matter is calculated from the condition of beta equilibrium, combined with the condition of a fixed Y_l,

$$\mu_p + \mu_e = \mu_n + \mu_{\nu_e} ,$$
$$Y_l = Y_e + Y_\nu , \qquad (1)$$

where μ_j are the chemical potentials of matter constituents. At the very initial stage we expect $Y_l \simeq 0.4$. Electron neutrinos are degenerate, with $\mu_{\nu_e} \gg T$ (in what follows we measure T in energy units). The deleptonization, implying the decrease of Y_l, occurs due to diffusion of neutrinos outward (driven by

the μ_{ν_e} gradient), on a timescale of seconds (Sawyer & Soni 1979, Bombaci et al. 1996). The diffusion of highly degenerate neutrinos from the central core is a dissipative process, resulting in a significant *heating* of the neutrino-opaque core (Burrows & Lattimer 1986).

2.2. Neutrino opaque core with $Y_\nu = 0$

This is the limiting case, reached after complete deleptonization. There is no trapped lepton number, so that $Y_l = Y_e$ and $Y_{\nu_e} = Y_{\bar{\nu}_e}$, and therefore $\mu_{\nu_e} = \mu_{\bar{\nu}_e} = 0$. Neutrinos trapped within the hot interior do not influence the beta equilibrium of nucleons, electrons and positrons, and for given n and T the equilibrium value of Y_e is determined from

$$\mu_p + \mu_e = \mu_n , \qquad (2)$$

while $\mu_{e^+} = -\mu_e$. In practice, this approximation can be used as soon as electron neutrinos become non-degenerate within the opaque core, $\mu_{\nu_e} < T$, which occurs after some ~ 10 seconds (Sawyer & Soni 1979, Bombaci et al. 1996). The neutrino diffusion is then driven by the temperature gradient, and the corresponding timescale of the heat transport (PNS cooling) can be estimated as $\sim 50(T/10 \text{ MeV})^{-3}$ s (Sawyer & Soni 1979).

2.3. Neutrinosphere and temperature profile

In principle, the temperature (or entropy per nucleon) profile within a PNS has to be determined via evolutionary calculation, starting from some initial state, and taking into account relevant transport processes in the PNS interior, as well as neutrino emission from PNS. Transport processes within neutrino-opaque interior occur on timescales of seconds, some three orders of magnitude longer than dynamical timescales. The very outer layer of PNS becomes rapidly transparent to neutrinos, deleptonizes, and cools on a very short timescale via $e^- e^+$ pair annihilation and plasmon decay. It seemed thus natural to model the thermal structure of the PNS interior by a hot core limited by a "neutrinosphere", and an outer envelope of $T < 0.5$ MeV. The transition through the "neutrinosphere" is accompanied by a temperature drop, which takes place over some interval of density just above the "edge" of the hot neutrino-opaque core, situated at some n_ν.

In view of the uncertainties in the actual temperature profiles within the hot interior of PNS, we considered two extremal situations for $n > n_\nu$, corresponding to an isentropic and an isothermal hot interior. In the first case, hot interior was characterized by a constant entropy per baryon $s = const.$. In the case of trapped lepton number, this leads to the EOS of the type: pressure $p = p(n, [s, Y_l])$, energy density $e = e(n, [s, Y_l])$, and temperature $T = T(n, [s, Y_l])$, with fixed s and Y_l. This EOS will be denoted by EOS$[s, Y_l]$. In the case of an isentropic, zero trapped lepton number EOS, we will have EOS$[s, Y_\nu = 0]$.

The condition of isothermality, which corresponds to thermal equilibrium, is more complicated. Due to the curvature of the space-time within PNS, the condition of isothermality corresponds to the constancy of $T^* = \frac{N}{\Gamma} T$ (see Sect. 3.1). The
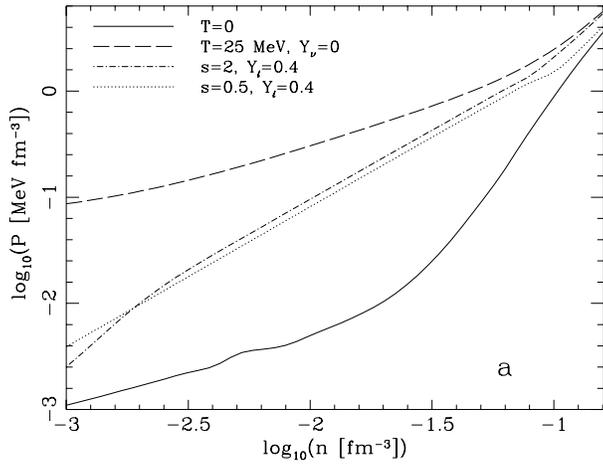
Fig. 1a. Pressure versus baryon density for our model of dense hot matter, under various physical conditions, for the subnuclear densities ($n < 0.16$ fm^{-3}). The curve $T = 0$ corresponds to cold catalyzed matter. The curve corresponding to $s = 0.5$, $Y_l = 0.4$ is unphysical, but has been added in order to visualize the importance of trapped lepton number at subnuclear densities.
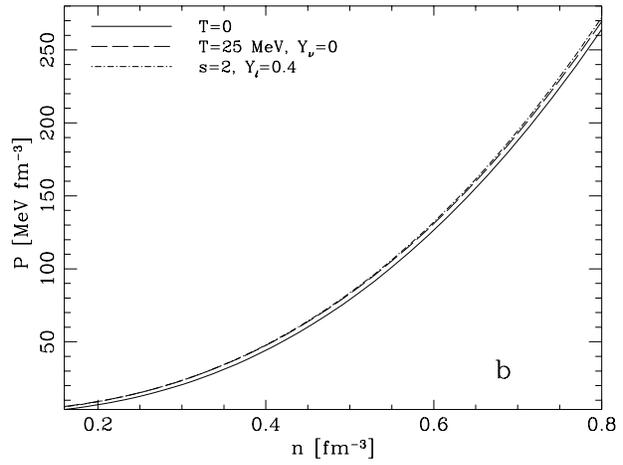
Fig. 1b. Pressure versus baryon density for our model of dense hot matter, under various physical conditions, for supranuclear densities ($n > 0.16$ fm^{-3}). Notation as in Fig. 1a.

significance of the $T^* = const.$ condition will be discussed in Sect. 3.1. In the static case, the isothermal state within the hot interior will be reached on a timescale corresponding to thermal equilibration, which is much longer than the lifetime of a PNS. In the case of a rotating PNS, the situation can be expected to be even more complicated (see, e.g., Chapter 8 of Tassoul (1978)). Nevertheless, we considered the $T^* = const.$ models for several reasons. First, as a limiting case so different from the $s = const.$ one, it enables us to check the dependence of our results for rapidly rotating PNS on the thermal state of the hot interior. Moreover, for the isothermal PNS we can apply the criterion of stability with respect to the axi-symmetric perturbations, and this will enable us to calculate the value of $\Omega_{\max}$ for the stable supramassive rotating PNS models with an isothermal interior (see Sect. 3).

Our calculation of the "neutrinosphere" within the hot PNS interior was done using a simple method, described below. For a given *static* PNS model, the neutrinosphere radius, R_ν, has been located through the condition

$$\int_{R_\nu}^{R} \frac{1}{\lambda_\nu(E_\nu)} \sqrt{|g_{rr}|} dr = 1 \;, \tag{3}$$

where λ_ν is the neutrino mean free path which is calculated at the matter temperature T, while E_ν is the mean energy of non-degenerate neutrinos at (and above) the neutrinosphere, $E_\nu = 3.15 T_\nu$. We assumed that opacity above R_ν is dominated by the elastic scattering off nuclei and nucleons, so that $\lambda_\nu = \lambda_\nu^0(n, T)/E_\nu^2$. Then, we determined the value of the density at the neutrinosphere, n_ν, for a given static PNS model, combining Eq. (3) with that of hydrostatic equilibrium, and readjusting accordingly the temperature profile within the outer layers of PNS. This value of n_ν was then used in the calculations of

rotating PNS models. Let us notice, that similar approximation, in which the "neutrinosphere" in rapidly rotating protoneutron star was defined as a surface of constant density, was used by Janka and Moenchmeyer (1989a, b). Some details concerning actual calculation of the temperature profile in the vicinity of the "neutrinosphere" will be given in Sect. 3.3.

2.4. Equation of state and static models of PNS

The starting point for the construction of our EOS for the PNS models was the model of hot dense matter of Lattimer and Swesty (1991), hereafter referred to as LS. Actually, we used one specific LS model, corresponding to the incompressibility modulus at the saturation density of symmetric nuclear matter $K = 220$ MeV. For $n > n_\nu$ we supplemented the LS model with contributions resulting from the presence of trapped neutrinos of three flavours (electronic, muonic and tauonic) and of the corresponding antineutrinos.

In Fig. 1a,b we show our EOS in several cases, corresponding to various physical conditions in the hot, neutrino-opaque interior of PNS. For the sake of comparison, we have shown also the EOS for cold catalyzed matter, used for the calculation of the (cold) NS models. In Fig. 1a we show EOS at subnuclear densities. At these densities, both the temperature and the presence of trapped neutrinos stiffen the EOS, as compared to the cold catalyzed matter one, and the stiffening is rather dramatic. The constant T EOS stiffens considerably at lower densities, which is due to the weak dependence of the thermal contribution (photons, neutrinos) on the baryon density of the matter (this effect will be to some extent moderated by the factor $\frac{\Gamma}{N}$ in the isothermal PNS, see Sect. 3.1). It is quite obvious, that $T = const.$ EOS becomes dominated by thermal effects below for $n < 10^{-2}$ fm^{-3}. On the contrary, for isentropic EOS, the effect of the trapped lepton number ($Y_l = 0.4$) turns out to be much more important than the thermal effects. This can be see in Fig.

1a, by comparing dash-dotted curve, [$s = 2$, $Y_l = 0.4$], with the dotted line, which corresponds to an artificial (unphysical) case with small thermal effects, [$s = 0.5$, $Y_l = 0.4$].

It is clear that the correct location of the "neutrinosphere", which separates hot interior from the colder outer envelope, should be important for the determination of the radius of PNS, and in consequence, of the maximum rotation frequency of a given PNS model.

It may be useful to compare our subnuclear EOS for PNS with those used by other authors. The subnuclear EOS of PNS, used in the papers of Hashimoto et al. (1995) and Bombaci et al. (1995, 96) is very different from that used in the present paper. In particular, Hashimoto et al. (1995) used a cold ($T = 0$) EOS for the densities below 10^{10} g cm^{-3}. On the other hand, Bombaci et al. (1995, 96) stop their hot EOS at the edge of the liquid interior, and use the $T = 0$ (cold catalyzed matter) EOS for the densities below 0.08 fm^{-3}; in this way, they seriously underestimate thermal and neutrino trapping effects on the radius of PNS.

Our EOS above nuclear density are plotted in Fig. 1b. The presence of a trapped lepton number softens the EOS, while thermal effects always stiffen it with respect to that for cold catalyzed matter. The softening of the supranuclear EOS at fixed Y_l is due to the fact that a significant trapped lepton number increases the proton fraction, which implies the softening of the nucleon contribution to the EOS.

It should be stressed, that in contrast to Hashimoto et al. (1995) and Bombaci et al. (1995, 96) we used a unified dense matter model, valid for both supranuclear and subnuclear densities. Also, the fact that we use various assumptions about the T and s profiles within PNS, enables us to study the relative importance of the temperature profile and that of a trapped lepton number, for the PNS models.

The mass-radius relation for the static PNS models calculated using various versions of our EOS for the hot interior is shown in Fig. 2. We assumed $n_\nu = 5 \times 10^{-3}$ fm^{-3}, which was consistent with our definition of the "neutrinosphere". For the sake of comparison, we show also the mass-radius relation for the $T = 0$ (cold catalyzed matter) EOS, which corresponds to cold neutron star models. In the case of the isothermal hot interior with central temperature $T_c = 25$ MeV we note a very small increase of the maximum mass, as compared to the $T = 0$ case (cf., Bombaci et al. 1995, 1996). However, the effect on the mass-radius relation is quite strong, and increases rapidly with decreasing stellar mass. In the case of the isentropic EOS with a trapped lepton number, [$s = 2$, $Y_l = 0.4$], the softening of the high-density EOS due to the trapped Y_l leads to the decrease of M_{max} compared to the $T = 0$ case; as far as the value of M_{max} is concerned, the softening effect of Y_l prevails over that of finite s (this is consistent with results of Takatsuka 1995 and Bombaci et al. 1995, 1996). However, the thermal effect on the radius is very important even in the case of $Y_l = 0.4$. This can be seen by comparing the [$s = 2$, $Y_l = 0.4$] curve with that corresponding to the unphysical, fictitious case of [$s = 0.5$, $Y_l = 0.4$].

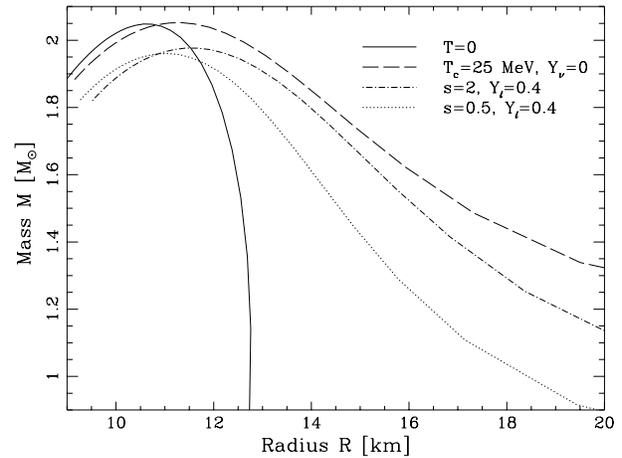The very initial state of a PNS corresponds to a significant trapped lepton number. With our assumption of a "standard"

Fig. 2. The gravitational mass versus stellar areal radius for static models of the protoneutron stars and neutron stars, under various assumptions concerning the physical conditions within the stellar interior. The curve corresponding to $s = 0.5$, $Y_l = 0.4$ is unphysical, but has been added in order to visualize the relative importance of the trapped lepton number and thermal effects. The curve $T = 0$ corresponds to cold neutron stars. The curve $T_c = 25$ MeV includes the $\frac{\Gamma}{N}$ factor.

composition of dense matter (i,e., excluding large amplitude K^--condensate, or a very large percentage of hyperons in cold dense matter), the maximum baryon mass (baryon number) of PNS is lower than that of cold NS. Therefore, in our case a stable PNS transforms into a stable NS, and the scenario PNS⟶Black Hole, considered by Baumgarte et al. (1996) is excluded.

At a given mass, the radius of a PNS is significantly larger than that of a cold NS. As remarked by Hashimoto et al. (1995), this should have important implications for rotating PNS. It should be stressed, however, that the value of radius, especially for PNS which are not close to the M_{max} configuration, turns out to be quite sensitive to the location of the edge of the hot neutrino-opaque interior (i.e., to the value of n_ν). The choice of Bombaci et al. (1996) would lead to a much smaller effect on R, while that of Hashimoto et al. (1995) would result in larger values of the PNS radii.

2.5. Stationarity

The EOS of PNS is evolving with time, due mainly to the deleptonization process, which changes the composition of matter, and also due to changes of the internal temperature of the star. However, these changes occur on the timescales $\tau_{evol} \sim 1$-10 s, which are three or more orders of magnitude longer than the dynamical timescale, governing the readjustment of pressure and gravity forces. This dynamical timescale $\tau_{dyn} \sim 1$ ms corresponds also to the characteristic periods of the PNS pulsations and of their rapid rotation. In view of this, we are able to decouple PNS evolution from its dynamics, and treat its rotation in the stationary approximation, with a well defined EOS of the PNS matter.

One of the neglected dynamical processes, implied by the radiative processes and the evolution of the thermal structure of a rotating PNS, is the meridional circulation of the matter. Strictly uniform rotation is incompatible with an assumption of a steady thermal state, resulting from the diffusive (radiative) equilibrium (see, e.g., Tassoul 1978). The requirement of radiative equilibrium will necessarily imply the existence of a meridional circulation of the matter. However, the velocity of this meridional circulation will be of the order of the stellar radius divided by the thermal timescale (the timescale of changes of the entropy of the PNS interior, which is of the order of neutrino diffusion timescale), which is much smaller than the rotational velocity (see, eg., Sect. 8 of Tassoul 1978). In view of this, we can neglect the effect of the meridional circulation when calculating the mechanical equilibrium of a rapidly rotating PNS. Finally, let us notice that in a special, idealized case of $T^* = const$, the radiative flux vanishes. Then, pure uniform rotation can be realized as a steady state of a PNS.

3. Formulation of the problem

The problem of the calculation of the stationary state of uniform rotation of cold neutron stars, within the framework of general relativity, was considered by numerous authors (see the review article of Friedman and Ipser 1992, and references therein). Extensive calculations for a broad set of realistic equations of state of cold dense matter were recently presented in (Cook et al. 1994) and (Salgado et al. 1994). Here, we will extend the methods used at $T = 0$ to the case of hot PNS. We will use the notation and formalism developed in the paper of Bonazzola et al. (1993), hereafter referred to as BGSM.

3.1. Equation of stationary motion

One of the problems introduced by finite temperature is that, if one does not make any other assumption about the equilibrium, the equation of stationary motion does not have a first integral (Bardeen 1972).

In the notation of BGSM, the equation of stationary motion (Eq. 3.25 of BGSM) reads, when the effects of temperature and rigid rotation are included, as

$$\partial_i(H + \ln \frac{N}{\Gamma}) = Te^{-H}\partial_i s \qquad (4)$$

where s is the entropy per baryon, T is the temperature, and $H = \ln[(e + p)/(nm_0c^2)]$ is the so-called pseudo-enthalpy (or log-enthalpy), N is the lapse function appearing in the space-time metric, and Γ is the Lorentz factor due to rotation. The equation of the stationary motion is to be supplemented with the equations determining the metric functions (see BSGM for the derivation and the explicit form of the complete set of equations).

In the expression for H, e is the energy density (which includes rest energy of matter constituents) and m_0 is the nucleon rest mass.

This equation is the general relativistic equivalent of a well-known Newtonian formula (see e.g. Tassoul 1978). It is straightforward to show that a *sufficient* condition for (4) to be integrable

is $T = T(n)$. In this case, one obtains a first integral of motion of the form :

$$H + \ln \frac{N}{\Gamma} - \int Te^{-H}ds = const. \qquad (5)$$

This enables us to calculate the density profile in the envelope of the PNS, because we have assumed a specific $T(n)$ profile within it (see Sect. 3.3). Let us stress that, due to the integral term in (5), the pseudo-enthalpy is no more an explicit function of the metric potentials, as it was in BGSM. In fact, one must solve (5) to have H within the star.

In the two particular cases, chosen by us for the hot interior, specific first integrals of Eq. (4) can be found. First, in the case of general relativistic thermal equilibrium, $T^* = T\frac{N}{\Gamma} = const.$, it is easy to show that

$$\mu^* = \mu \frac{N}{\Gamma} = const., \qquad (6)$$

where $\mu = (e + p)/n - Ts$ is the baryon chemical potential, is indeed the integral of (4). The constancy of T^* and μ^* corresponds to the general-relativistic thermodynamic equilibrium, if we neglect the time dependence of the EOS of PNS (i.e., if we freeze transport phenomena). Second, in the case of isentropic profile $s(n, T(n)) = const.$, the thermal term in (4) vanishes and the first integral of Eq. (4) reads

$$T^*s + \mu^* = const. \qquad (7)$$

3.2. Instabilities and maximum mass

The instabilities that could develop in rapidly rotating PNS, and which could limit the maximum angular frequency of these objects, are of secular and of dynamic type.

Let us start with the problem of secular stability with respect to the axi-symmetric perturbation of rotating configurations. We denote the total baryon number, total angular momentum, and total entropy of a PNS by N_{bar}, J, and S, respectively. We used the *secular* instability criterion of Friedman et al. (1988), extended to the case of finite temperature. For the purpose of completeness, we restate here their lemma (and correct a misprint of their paper).

Lemma : Consider a three-parameter family of uniformly rotating hot stellar models having an equation of state of the form $p = p(e, T)$. Suppose that along a continous sequence of models labelled by a parameter λ, there is a point λ_0 at which $\dot{N}_{bar} = dN_{bar}/d\lambda$, $\dot{J}$ and $\dot{S}$ vanish and where $\frac{d}{d\lambda}(\mu^*\dot{N}_{bar} + \dot{\Omega}\dot{J} + \dot{T}^*\dot{S}) \neq 0$. Then the part of the sequence for which $\mu^*\dot{N}_{bar} + \dot{\Omega}\dot{J} + \dot{T}^*\dot{S} > 0$ is unstable for λ near λ_0.

Similarly as in the case of Friedman et al. (1988), this lemma follows directly from Theorem I of Sorkin (1982), with his function S replaced by $-M$, the E^α quantities replaced by N_{bar}, J, S and the β^α ones by μ^*, Ω, T^*. The conditions of the theorem are fulfilled because stellar models are configurations for which M is minimized at fixed N_{bar}, J and S, *and* because difference

in M between two neighbouring equilibria can be expressed as (Bardeen 1970)

$$dM = \mu^{\star} dN_{\mathrm{bar}} + \Omega dJ + T^{\star} dS. \tag{8}$$

Let us stress here that this last equation requires either $T^{\star}$ or s to be constant through the whole star, which fixes, in each of these two cases, the temperature profile within the stellar model.

We investigated the stability of our models with a specific version of this criterion, in which we choose a continous sequence of equilibria to be a sequence at fixed N_{bar} and S. The point of the loss of stability is then simply the point of extremal J, i.e. :

$$\left(\frac{\partial J}{\partial \rho_{\mathrm{c}}} \right)_{N_{\mathrm{bar}}, S} = 0, \tag{9}$$

where ρ_{c} is the central density of the star.

The instability discussed above is a secular one; it will develop on the timescale needed to transport the angular momentum within the perturbed model, in order to decrease the energy of the star while changing its shape and structure. However, the timescale of the PNS evolution is quite short (seconds), and it is driven by the same transport processes involving neutrinos, as those which are needed to destabilize the star via the axi-symmetric perturbations. In view of this, one might expect that the secular instability described above is not efficient in disrupting the quasi-stationary configuration of rapidly rotating PNS.

However, we should remember that the above considerations apply to the case of infinitesimal perturbations. Transport processes would be crucial for removing the energy barrier separating the initial, secularly unstable configuration, from the dynamically unstable one, which would eventually collapse into a black hole. However, newly born PNS are expected to be in a highly excited state, in which various modes of stellar pulsations are excited. One may expect that the energy contained in these pulsations is sufficient to overcome the energy barrier separating the actual metastable, secularly unstable state from the dynamically unstable, collapsing one. In view of this, we expect that the secularly unstable configurations should be treated like unstable ones. Therefore, the critical configuration, given by Eq.(9), will be thus considered as the last stable one.

A rapidly rotating PNS can be also susceptible to other types of secular instabilities. The instability with respect to the non axisymmetric perturbations can be driven by the gravitational radiation reaction (GRR). However, detailed calculations performed for hot NS suggest, that at the temperature exceeding 10^{10} K these instabilities can only slightly decrease the maximum rotation frequency of uniform rotation, due to the damping effect of the matter viscosity (Cutler et al. 1990, Ipser & Lindblom 1991, Lindblom 1995, Yoshida & Eriguchi 1995, Zdunik 1996). Secular instabilities of rapidly rotating NS with respect to the non-axisymmetric "bar" mode were recently investigated by Lai & Shapiro (1995) and Bonazzola et al. (1995). While Lai & Shapiro (1995) addressed the problem of "bar" instability of newly formed NS, they assumed a rather unrealistic "ellipsoidal

model", involving only shear viscosity as a source of viscous dissipation, and performed their calculations within the Newtonian theory of gravity. On the other hand, in their relativistic calculations Bonazzola et al. (1995) considered only cold NS, and found that the secular "bar" instability can set in before the Keplerian (mass shedding) limit is reached only for sufficiently stiff EOS of NS matter. The problem of the "bar" instability of PNS, with realistic EOS of the hot interior, will be investigated by us in the future. In any case, inclusion of possible additional secular instabilities can only decrease the maximum rotation frequency of PNS below the values obtained using the simplified approach adapted in the present paper.

The fact of the existence of the maximum mass of rotating PNS, $M_{\mathrm{max}}^{(\mathrm{rot})}$ (and maximum baryon mass, $M_{\mathrm{bar,max}}^{(\mathrm{rot})}$) (see Sect. 5), puts a well defined and stringent limit on Ω_K which can be reached by PNS. Configurations with $M_{\mathrm{bar}} > M_{\mathrm{bar,max}}^{(\mathrm{rot})}$ are *dynamically unstable*: no stationary solution exists above $M_{\mathrm{bar,max}}^{(\mathrm{rot})}$. At the same time, the angular frequency of rigid rotation cannot exceed the Keplerian value, Ω_K. These two conditions, combined with the instability criterion, expressed in Eq. (9), determine the maximum frequency (or, strictly speaking, an upper bound on the frequency) of rigid rotation of PNS. Practical implementation of these criteria will be described in Sect. 5.

3.3. Isothermal and isentropic temperature profiles

A consistent study of PNS would require an exact treatment of the thermal transport in the frame of a non-stationary spacetime. Unfortunately, such a study is beyond the scope of the present work, and we have thus chosen to impose "by hand" the temperature profile within the star, following prescription described in Sect. 2.3. We divided the interior of PNS into the hot interior ($n > n_{\nu}$), a layer corresponding to the temperature drop within the "neutrinosphere" ($n_{\nu} - \Delta n_{\nu} < n < n_{\nu}$), and the low temperature, neutrino-transparent outer envelope with $n < n_{\nu} - \Delta n_{\nu}$. We have chosen two types of temperature profiles within the hot, neutrino-opaque core ($n > n_{\nu}$) :

– the isothermal profile : $T = T^{\star} \frac{\Gamma}{N}$, with $T^{\star} = const.$,

– the isentropic profile : $T = T(n)$, with $s(n, T(n)) = const.$

For the transition region and the low temperature envelope, we used a suitable profile $T(n)$:

$$T(n) = 0.2 \text{ MeV for } n < n_{\nu} - \Delta n_{\nu}$$
$$T(n) = f(n) \text{ for } n_{\nu} > n > n_{\nu} - \Delta n_{\nu}.$$

The function f was chosen for computational convenience as a suitable combination of an exponential and a gaussian function, selected to lead to $T(n)$ of class $\mathscr{C}^1$ through the transition (temperature drop) region. Our typical choice was $\Delta n_{\nu}/n_{\nu} = 2 \ 10^{-2}$; increasing this value up $\Delta n_{\nu}/n_{\nu} = 0.2$ led to a very small increase of the stellar radius.

As the mass of a massive PNS is almost entirely contained in the hot neutrino-opaque core (a rough estimate for a typical star gives less than 10^{-3} of the total mass for the cool envelope

mass), we supposed that our stability criterion remained valid also in the case of the presence of the low temperature envelope.

4. Numerical method

We used a code based on the 3 + 1 formulation of the Einstein equations in stationary axisymmetric spacetimes (BGSM). The four elliptic equations obtained were solved by means of a spectral method, in which the functions are expanded in different polynomial bases (Chebyshev for r, Legendre for θ and Fourier for ϕ). We refer the reader to BGSM for a detailed description of the code, including the description of the "virial" indicator used for monitoring the convergence and the precision reached. Let us just say that the code was modified to take into account thermal effects and, contrary to Salgado et al. (1994), to converge to the solution with various quantities being held fixed (for example $M_{\rm bar}$ or J or S). Here we briefly outline some of the numerical checks we made.

The two-parameters EOS was interpolated using bicubic splines subroutine from the NAG library. In this way, the thermodynamic functions are of class $\mathscr{C}^2$, but the thermodynamic consistency is not conserved.

The global relative error, evaluated by the means of the virial check (see BGSM), is $\sim 2 \cdot 10^{-3}$. This relatively "low" precision is due to the thermodynamical inconsistencies.

We used two grids in r for the star and one in $1/r$ for the exterior with $N_r = 33$ in each, and one grid in θ with $N_\theta = 17$. We checked that a greater N_r or N_θ does not change the results by more than a few 10^{-4} at most, which stays within the global precision reached. Let us stress that such a low number of grid points is sufficient to reach high accuracy within a spectral method (that would not be the case with a finite difference scheme).

The temperature drop at the "neutrinosphere" is not always located on the border of the internal grid in r, which could influence the precision (remember that the spectral methods are very sensitive to discontinuities). We checked that, in fact, even when the "neutrinosphere" is far from the border of the grid, the global physical quantities of the star did not change much (we found also relative variations of a few 10^{-4} at most).

For a "simple" model where (T_c, ρ_c, Ω_c) were held fixed, convergence required no more than 50 iterations and ~ 1 minute of CPU time on a Silicon Graphix Indigo^2 workstation. However, the number of iterations can reach 400 if one needs to converge to, e.g., a Keplerian configuration at fixed supra-massive baryon mass.

Finally, we compared our results at $T = 0$ and $\Omega = 0$ with the results of another code used by one of us (P. Haensel), and found that the relative differences in the global properties of the stellar models are of the order of $\sim 10^{-3}$, which can be imputed to the different interpolation procedures.

5. Numerical results. Maximally rotating protoneutron stars

For a given EOS, rapidly rotating PNS models can be divided into two families: normal and supramassive one. Normal models
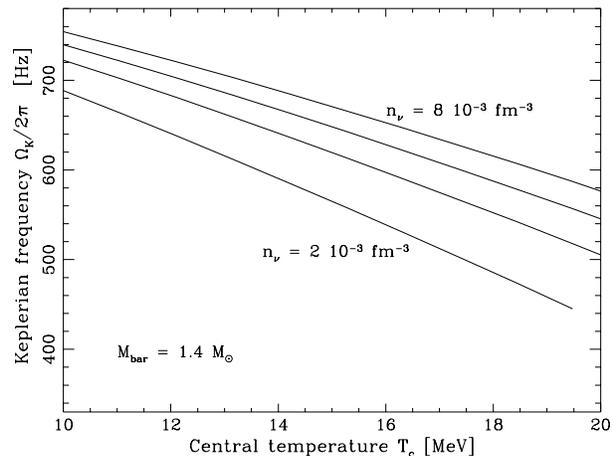

Fig. 3. The value of the Keplerian frequency, $\Omega_K/2\pi$, versus central temperature, T_c, for protoneutron star models with an isothermal, neutrino opaque, $Y_\nu = 0$ (zero trapped lepton number) hot core. The baryon mass of rotating models is fixed at $M_{\rm bar} = 1.4\ M_\odot$. Different lines correspond to different values of the nucleon density at the edge of the hot core, n_ν. The value of n_ν increases by $2\ 10^{-3}$ fm^{-3} when going upwards from one line to the next one.

are those with baryon mass which does not exceed the maximum allowable baryon mass of static (non-rotating) configurations, $M_{\rm bar,max}^{\rm (stat)}$. A *normal* rotating model can be transformed into a static configuration of the same baryon mass, through a continuous decrease of Ω. Rotation of PNS increases their maximum allowable mass with respect to the static case, up to $M_{\rm bar,max}^{\rm (rot)}$. Rotating PNS models with $M_{\rm bar,max}^{\rm (stat)} < M_{\rm bar} < M_{\rm bar,max}^{\rm (rot)}$ are called *supramassive*. Such a supramassive rotating model cannot transform into a static model, because in the process of decreasing angular velocity it will collapse into a black hole.

The maximum angular velocity of the normal and supramassive rotating models results from different stability conditions. In the case of normal rotating configurations the value of Ω is bound by the mass shedding limit, which corresponds to the Keplerian velocity at the stellar equator, $\Omega_K(M_{\rm bar})$. The value of Ω_K turns out to be rather sensitive to the location of the "neutrinosphere" within the PNS. This sensitivity is particularly large in the case of the isothermal profile of the hot neutrino-opaque core. This is visualized in Fig. 3, where we show the dependence of the mass shedding limit Ω_K for PNS with baryon mass 1.4 $M_\odot$ on the value of n_ν, for the central temperatures ranging between 10 and 20 MeV. The dependence on the value of n_ν weakens with increasing $M_{\rm bar}$. Also, this effect is much less important in the case of isentropic PNS.

For supramassive rotating PNS, the limit on Ω has been set by the condition of stability of rotating models with respect to the axi-symmetric perturbations, which was combined with the mass shedding stability condition. Our calculations have been performed for both isothermal ($T^* = const.$) and isentropic ($s = const.$) hot interiors of PNS. In both cases, the absolute maximum of Keplerian frequency for rotating models, which were stable with respect to the axi-symmetric perturba-
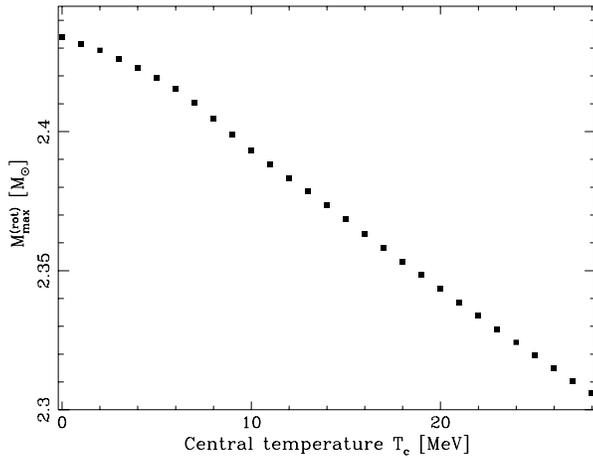
Fig. 4a. Maximum gravitational mass of rotating protoneutron star models with isothermal cores and $Y_\nu = 0$ (zero trapped lepton number), versus central temperature, T_c. The nucleon density at the outer edge of the hot core $n_\nu = 5\ 10^{-3}\ \mathrm{fm}^{-3}$.
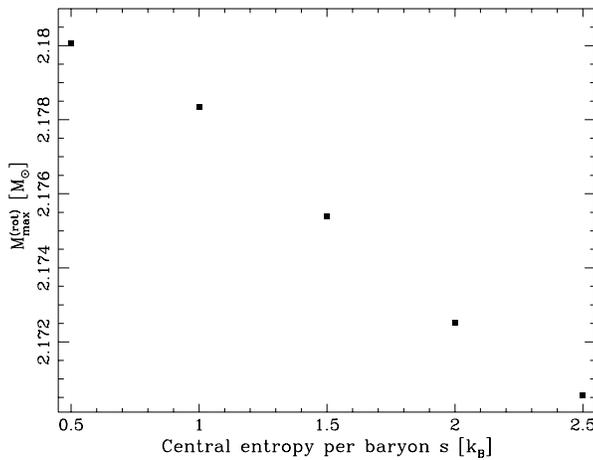

Fig. 4b. Maximum gravitational mass of rotating protoneutron star models with isentropic hot cores with $Y_l = 0.4$, versus central entropy, s. The nucleon density at the outer edge of the hot core is $n_\nu = 5\ 10^{-3}\ \mathrm{fm}^{-3}$.

tions, was obtained for a rotating configuration with a maximum baryonic mass (and gravitational mass), $M_{\mathrm{bar,\ max}}^{(\mathrm{rot})}$ $[M_{\mathrm{max}}^{(\mathrm{rot})}]$. Actually, rotating configuration with $M_{\mathrm{max}}^{(\mathrm{rot})}$ and that with Ω_{max} do not generally coincide (see, e.g., Cook et al. 1994, Stergioulas & Friedman 1995). However, the difference is very small, and it could not be detected within the precision of our numerical code. The value $M_{\mathrm{max}}^{(\mathrm{rot})}$ depends on the value of T^* in the case of isothermal hot interior, but we preferred to parametrize it in terms of central temperature, $T_c \equiv T(r = 0)$. The dependence of $M_{\mathrm{max}}^{(\mathrm{rot})}$ on the value of T_c is displayed in Fig. 4a. The effect of temperature on $M_{\mathrm{max}}^{(\mathrm{rot})}$ is opposite to that seen for $M_{\mathrm{max}}^{(\mathrm{stat})}$: thermal effects lower the value of $M_{\mathrm{max}}^{(\mathrm{rot})}$ as compared to that for cold neutron stars. This is due to the thermal increase of the equatorial radius, which prevails over the thermal stiffening of the

Table 1. Parameters of the static and rotating maximum mass configurations of protoneutron stars

EOS	$M_{\mathrm{max}}^{(\mathrm{stat})}$ [$M_\odot$]	$R_{\mathrm{max}}^{(\mathrm{stat})}$ [km]	$M_{\mathrm{max}}^{(\mathrm{rot})}$ [$M_\odot$]	$R_{\mathrm{max}}^{(\mathrm{rot})\,a}$ [km]	$\Omega_{\mathrm{max}}/2\pi$ [Hz]
$T = 0,\ Y_\nu = 0$	2.048	10.59	2.430	14.34	1625
$T_c = 25,\ Y_\nu = 0$	2.053	11.17	2.322	14.79	1521
$s = 0.5,\ Y_l = 0.4$	1.957	10.85	2.180	14.40	1522
$s = 2,\ Y_l = 0.4$	1.977	11.53	2.172	15.32	1388

[a] Equatorial radius of maximaly rotating configuration.

central core of PNS. The dependence of $M_{\mathrm{max}}(\mathrm{rot})$ on the value of s in the case of isentropic hot interior of PNS is represented in Fig. 4b, in the case of $Y_\nu \neq 0$ (trapped lepton number) and for $Y_l = 0.4$. The decrease of $M_{\mathrm{max}}(\mathrm{rot})$ is there smaller than in the case of the isothermal PNS models.

In Fig. 5a,b we show our results for the maximum rotation frequency of stable PNS models, reached for supramassive configurations. In the case of the isothermal PNS, thermal effects tend to decrease the value of Ω_{max}, but even in the case of $T_c = 25$ MeV the relative effect does not exceed ten percent. Irregularities at lower T_c result from the limited accuracy of determination of the critical configuration with an isothermal core.

Maximum rotation frequency in the case of the isentropic hot neutrino-trapped cores of PNS is shown, for several values of the central entropy per baryon, in Fig. 5b. The value of Ω_{max} is also decreasing with increasing s.

In general, we find that the decrease of Ω_{max}, as compared to cold neutron stars, is in our case smaller than that found by Hashimoto et al. (1995); this may be due to the lower value of the density at the edge of the hot core, assumed by these authors. Some differences may also be due to different supranuclear EOS, and to a different treatment of the thermal effects, in particular, to their assumption of $T = const.$. In order to visualize the importance of the relativistic effects on $T(r)$ in the isothermal interior of a PNS, we show in Fig. 6 the temperatures $T(r)$ and T^*, for $M_{\mathrm{bar}} = 1.5\ M_\odot$, and a uniform Keplerian rotation. As one can see, in the central part of the PNS, T is about 30 percent greater than T^*. A similar effect is seen also in the case of an isentropic hot interior, which in Fig. 6 corresponds to $s = 2,\ Y_l = 0.4$.

6. Empirical formula for Ω_{max}

The calculation of the rotating PNS (and NS) models is incomparably more difficult than that of the static models. In the case of cold NS, one finds a surprisingly precise universal formula, which relates the maximum rotation frequency to the mass and radius of the maximum mass configuration for the static models
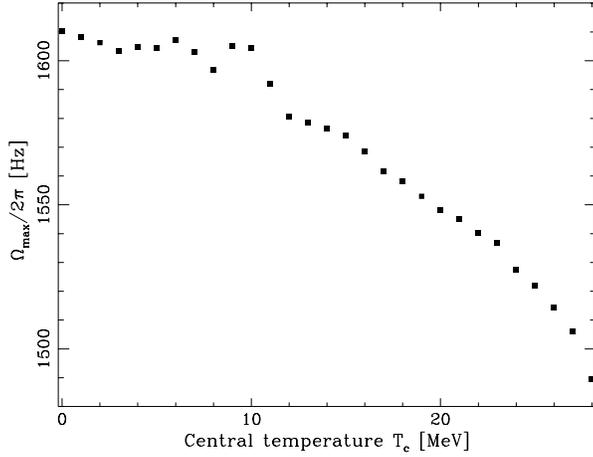
Fig. 5a. Maximum rotation frequency of stable protoneutron star models with isothermal hot cores (with zero trapped lepton number), versus central temperature, T_c. The nucleon density at the outer edge of the hot core is $n_\nu = 5 \ 10^{-3} \ \mathrm{fm}^{-3}$.
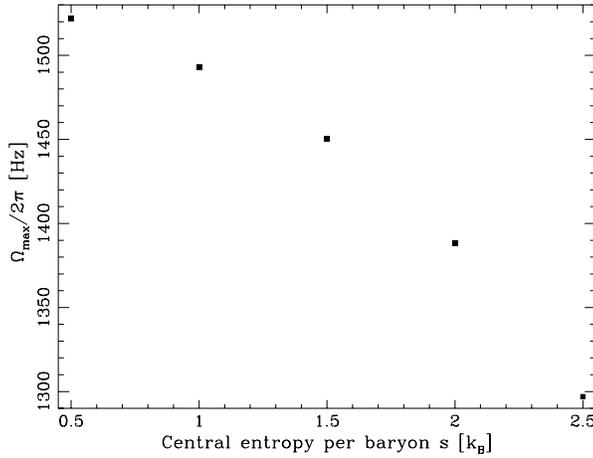

Fig. 5b. Maximum rotation frequency of stable protoneutron star models with isentropic hot cores with $Y_l = 0.4$, versus central entropy, s. The nucleon density at the outer edge of the hot core is $n_\nu = 5 \ 10^{-3} \ \mathrm{fm}^{-3}$.

(Haensel & Zdunik 1989, Friedman at al. 1989, Shapiro et al. 1989, Haensel et al. 1995, Nozawa et al. 1996),

$$\Omega_{\max} = C \left(\frac{M_{\max}^{(\mathrm{stat})}}{M_\odot} \right)^{\frac{1}{2}} \left(\frac{R_{\max}^{(\mathrm{stat})}}{10 \ \mathrm{km}} \right)^{-\frac{3}{2}} , \tag{10}$$

where the most recent value of C, based on calculations performed for a broad set of realistic *cold* EOS of dense matter, is $C_{\mathrm{cold}} = 7750 \ s^{-1}$ (Haensel et al. 1995). The "empirical formula", Eq. (10), reproduces the values of $\Omega_{\max}$ for cold NS models with typical precision better than 5% (although in some specific cases the deviations can reach nearly 7%, see Nozawa et al. 1996).

The validity of the empirical formula for $\Omega_{\max}$ is of great practical importance. For cold EOS of dense matter, it enables
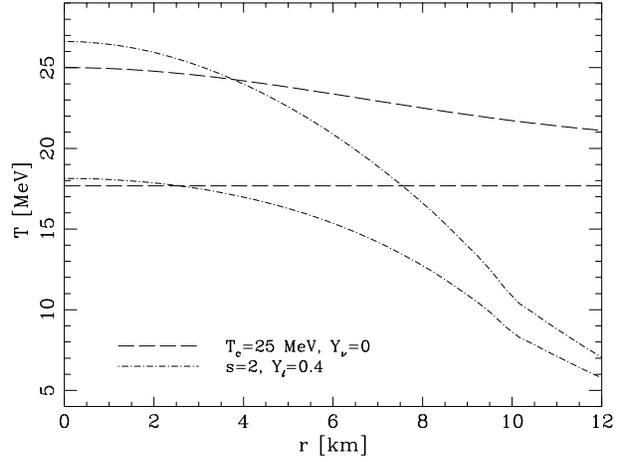

Fig. 6. Difference between T and T^* in the hot interior of a $M_{\mathrm{bar}} = 1.5$ $M_\odot$ PNS in Keplerian rotation, for the two models of the hot PNS core. Dashed lines correspond to the isothermal ($T_c = 15$ MeV), and the dash-dot lines to the isentropic model, respectively. For each pair of curves, upper one corresponds to $T(r)$, and the lower one to $T^*(r)$. Temperatures are plotted versus radial coordinate r in the equatorial plane of rotating PNS.

one to get immediately a rather precise estimate of the value of $\Omega_{\max}$, using easily calculated static neutron star models, and avoiding in this way incomparably more difficult 2-D calculations of rotating NS models and the analysis of their stability.

It is of interest to check, whether "empirical formula" is valid also in the case of hot PNS. Let us notice, that the subnuclear EOS of PNS, with possible lepton number trapping, is very different from that of cold catalyzed matter (see Fig. 1). In order to check the validity of the empirical formula, we define the EOS depending parameter C_{EOS},

$$C_{\mathrm{EOS}} \equiv \Omega_{\max} \left(\frac{M_{\max}^{(\mathrm{stat})}}{M_\odot} \right)^{-\frac{1}{2}} \left(\frac{R_{\max}^{(\mathrm{stat})}}{10 \ \mathrm{km}} \right)^{\frac{3}{2}} , \tag{11}$$

where the right-hand-side is calculated using exact results for a specific EOS. The values of C_{EOS} for our models of PNS are displayed in Fig. 7a,b. Let us notice, that for isentropic hot cores with trapped lepton number the value of C_{EOS} shows a decreasing trend with increasing s. In the case of isothermal hot cores with $Y_\nu = 0$ we see the opposite trend: the value of C_{EOS} tends to increase with central temperature. The value of $C_{\mathrm{hot}} = 7800 \ s^{-1}$ will lead to a very good empirical formula for PNS, with precison comparable to that used for cold NS. Within the precision of the empirical formulae, the values of C_{cold} and C_{hot} can be considered as being equal.

7. Numerical results. From hot protoneutron stars to cold neutron stars

Rapidly rotating hot, neutrino-opaque PNS evolves eventually into a cold, rotating NS, which under favourable circumstances can be observed as a solitary pulsar. Let us assume, that such

Table 2. Maximum rotation frequencies and maximum baryon masses of PNS with various EOS, and corresponding frequencies of cold NS configurations, obtained via cooling at constant J and $M_{\rm bar}$ (J-losses due to neutrino emission are neglected).

EOS	$M_{\rm bar,max}^{\rm (rot)}$ $[M_\odot]$	$\Omega_{\rm max}^{\rm (hot)}/2\pi$ [Hz]	$\Omega_{\rm max}'^{\rm (cold)}/2\pi$ [Hz]
$T_c = 9, Y_\nu = 0$	2.806	1603	1582
$T_c = 25, Y_\nu = 0$	2.695	1521	1403
$s = 2, Y_L = 0.4$	2.172	1388	1112

a transformation took place at constant baryon mass: this assumption is valid if mass accreted after the formation of a PNS is negligibly small. (Notice, that we can *define* the moment of formation of a PNS as that at which the accretion ends). Second assumption refers to the angular momentum of the star. Let us neglect for the time being the angular momentum loss due to emission of neutrinos (mainly during deleptonization), as well as that due to gravitational radiation (if rotating star deviated from the axial symmetry). Inclusion of both effects could only *decrease* the final angular momentum of the NS. Under these two assumptions, the transformation of a PNS into a solitary radio pulsar takes place at constant baryon mass, $M_{\rm bar}$, and angular momentum, J. The maximum angular frequency of a solitary radio pulsar of a given baryon mass would be then determined by the parameters of a maximally rotating PNS of the same baryon mass.

In the present paper we restrict ourselves, similarly as Hashimoto et al. (1995), to the case of rigid rotation of PNS. We will first consider "typical" range of baryon masses expected for the NS born in a gravitational collapse of a massive stellar core, $1.4\,M_\odot < M_{\rm bar} < 2.0\,M_\odot$ (for our EOS of dense matter this would correspond to $1.3\,M_\odot \lesssim M \lesssim 1.8\,M_\odot$). All stars considered are normal, and the maximum initial frequency of PNS will be then $\Omega_K[{\rm hot}, Y_\nu = 0]$, and $\Omega_K[{\rm hot}, Y_l = 0.4]$, for the limiting case of the zero trapped lepton number, and maximum trapped lepton number neutrino-opaque cores, respectively. The values of these limiting angular frequencies, for the isothermal and isentropic PNS cores, are plotted versus $M_{\rm bar}$ in Fig. 8 (thin dashed and dash-dotted lines, respectively).

Our results displayed in Fig. 8 lead to some conclusions, relevant to those neutron stars which remained solitary after their birth in the gravitational collapse of a massive stellar core. If the starting configuration (at the end of significant accretion, after the revival of a stagnated shock) was that with trapped lepton number and isentropic, then the maximum frequency of such a neutron star, in the gravitational mass range of 1.3 - 1.8 $M_\odot$, cannot exceed 600 - 900 Hz, the lower frequency limit corresponding to the lower mass limit. The corresponding range of minimum periods would be from 1.6 ms to 1.1 ms, respectively.
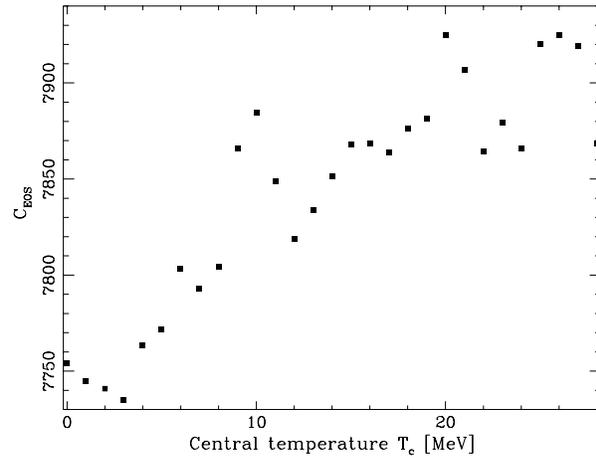

Fig. 7a. The coefficient $C_{\rm EOS}$, given by Eq.(11), versus central temperature, T_c, for isothermal models of the zero trapped lepton number ($Y_\nu = 0$) hot cores of protoneutron stars.
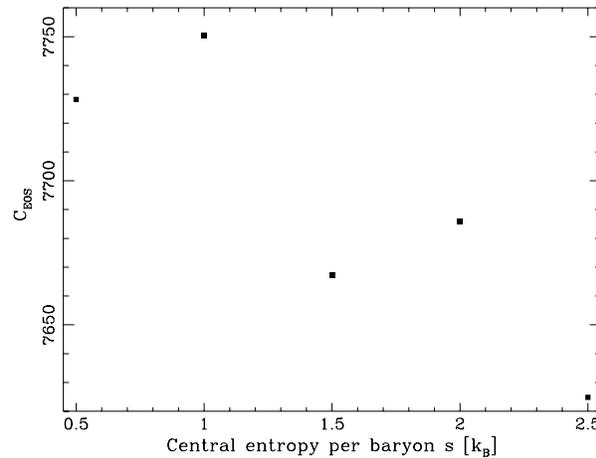

Fig. 7b. The coefficient $C_{\rm EOS}$, given by Eq.(11), versus central entropy per nucleon, for isentropic $Y_l = 0.4$ models of hot cores of protoneutron stars.

If the "initial isolated configuration" (i.e., that with no subsequent accretion) was a little older, and therefore deleptonized, and if we assume that it was isothermal, then the resulting constraints would be less stringent: for the range of masses 1.3 - 1.8 $M_\odot$ we get minimum rotation periods of 1.25 - 1.1 ms, respectively.

In both cases cooling resulted in speeding up of the rotation of the star: such situation is characteristic of "normal rotating models".

Similar evolutionary considerations can be applied to the "maximally rotating configurations": isentropic one with $s = 2$, $Y_l = 0.4$ and isothermal ones with $T_c = 9$ MeV, 25 MeV, respectively. Our results are shown in Table 2. The initial "hot" configurations are supramassive, and evolve into more compact cool ones (at constant $M_{\rm bar}$ and J) *decreasing* their angular frequency (slowing down). This purely relativistic effect was re-
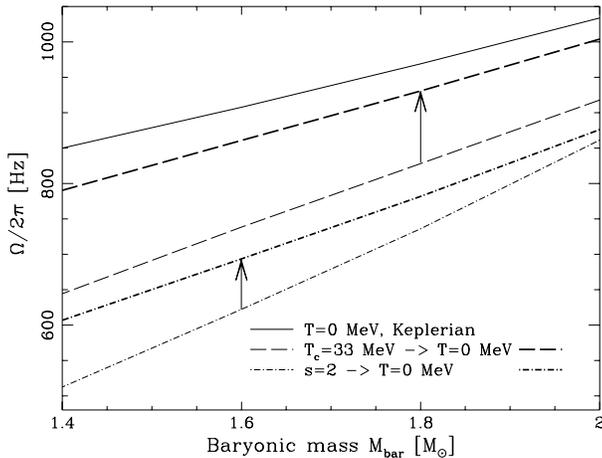
Fig. 8. Maximum rotation frequencies versus baryon mass of rotating configurations. Solid line: maximum rotation frequencies of cold neutron star models, $\Omega_K(\text{cold})$. Thin dashed line: maximum rotation frequency for isothermal models with $T_c = 33$ MeV with no trapped lepton number ($Y_\nu = 0$), denoted in the text as $\Omega_K[\text{hot}, Y_\nu = 0]$. Heavy dashed line: angular frequency of cold configurations, resulting from those corresponding to thin dashed line by cooling at constant J and M_{bar}. Thin dash-dotted line: maximum rotation frequency for isentropic models, denoted in the text as $\Omega_K[s = 2, Y_l = 0.4]$. Heavy dash-dotted line: angular frequency of cold configurations, resulting from those corresponding to thin dash-dotted line by cooling at constant J and M_{bar} (J-losses due to neutrino emission are neglected).

cently pointed out by Hashimoto et al. (1995). The "relativistic slowing down" during cooling of the maximally rotating isentropic configuration with $s = 2$, $Y_l = 0.4$ corresponds to the increase of the period from $P_{\min}[s = 2, Y_l = 0.4] = 0.72$ ms up to $P'_{\min} = 0.90$ ms. If such a scenario of formation of solitary pulsars is valid, an absolute limit on their period would be $P'_{\min}$, and not $P_{\min}(T = 0) = 0.61$ ms, obtained for the $T = 0$ EOS. The slowing down factor of $\simeq \frac{2}{3}$ coincides with that obtained by Hashimoto et al. (1995) for a different EOS and a different scenario of formation of solitary cold pulsars. Actually, they assumed that the initial configuration is that with $T = const., Y_\nu = 0$. Their initial model would to some extent correspond to our isothermal models (remember however the factor $\frac{N}{\Gamma}$ in our temperature profiles, which is absent in their calculations). Using Tables 1, 2 we obtain $P'_{\min}[T_c = 25, Y_\nu = 0]/P_{\min}[T = 0] = 0.92$, which is quite close to 1.

8. Discussion and conclusions

In the present paper we studied rapid rotation of protoneutron stars, using a specific model of hot, dense matter. Our models of rapidly rotating protoneutron stars were based on several simplifications, which were necessary in order to make the problem tractable. In order to avoid difficulties and/or ambiguities of the largely unknown "real situation", we restricted ourselves to studying idealized, limiting cases. In many places we introduced

approximations, which were crucial for making numerical calculations feasible.

We assumed rigid rotation within protoneutron star. This simplified greatly our considerations, and reduced dramatically the number of stellar models. Actually, our formalism allows calculation of the quasi-stationary differentially rotating configurations, after introducing an additional $F \partial_i \Omega$ term appearing on the right hand side of the equation of stationary motion, Eq. (4) (see Sect. 5.1 of BGSM). We plan to perform studies of differentially rotating protoneutron stars in the near future, as the next step in our investigations of dynamics of protoneutron stars. While existing numerical simulations of gravitational collapse of rotating cores of massive stars yield a differentially rotating protoneutron star, the calculations stop too early after bounce. In contrast to our models of protoneutron stars, the object which comes out from the simulations of Moenchmeyer and Mueller has an extended, very hot envelope, produced by the shock wave immediately after bounce (Janka & Moenchmeyer 1989a,b, Moenchmeyer & Mueller 1989). Also, the lack of knowledge of the initial angular velocity distribution within the collapsing core results in the uncertainty in the rotational state of produced protoneutron star. Clearly, the study of quasistationary differential rotation of protoneutron stars should take into account all these uncertainties.

Deleptonization of protoneutron star is connected with energy and angular momentum losses. However, angular momentum taken away by neutrinos is expected to constitute at most a few percent of the total stellar angular momentum (Kazanas 1977). Inclusion of this effect would slightly decrease some of our "evolutionary limits" of Sect. 7.

Our treatment of the thermal state of the protoneutron star interior should be considered as very crude. The temperature profile might be affected by convection. Also, our method of locating the "neutrinosphere" was very approximate. Clearly, the treatment of thermal effects can be refined, but we do not think this will change our main results.

Our calculations were performed for only one model of the nucleon component of dense hot matter. The model was realistic, and enabled us to treat in a unified way the whole interior (core as well as the envelope) of the protoneutron star. However, in view of the uncertainties in the EOS of dense matter at supranuclear densities, one should of course study the whole range of theoretical possibilities, for a broad set - from soft to stiff - of supranuclear, high temperature EOS. An example of such an investigation, in the case of the *static* protoneutron stars, is the study of Bombaci et al. (1996). In view of the possible importance of the protoneutron star - neutron star connection for the properties of solitary pulsars, similar studies should also be done for rotating proto-neutron stars.

The calculations of the present paper were done under the assumption, that the frequency of uniform rotation of protoneutron stars is limited only by the mass shedding and the secular instability with respect to the axi-symmetric perturbations. In view of this, our results can be considered only as upper bounds to the maximum rotation frequency. Our main conclusion is that the minimum rotation period of solitary neutron stars, born as

rapidly rotating protoneutron stars, is significantly larger, than the corresponding limit for cold neutron stars. Inclusion of additional secular instabilities in rapidly, uniformly rotating protoneutron stars can only strengthen this conclusion.

References

Bardeen J.M., 1970, ApJ, 162, 71

Bardeen J.M., 1972, in "Black Holes - Les astres occlus", Les Houches, ed. De Witt C. & De Witt B.S., Gordon and Breach Sci. Pub., New York

Baumgarte T.W., S.L. Shapiro, S.A. Teukolsky, 1996, ApJ 458, 680

Bombaci I., Prakash M., Prakash M., Ellis P.J., Lattimer J.M., Brown G.E., 1995, Nucl. Phys. A, 583, 623

Bombaci I., 1996, A&A 305, 871

Bombaci I., Prakash M., Prakash M., Ellis P.J., Lattimer J.M., Brown G.E., 1996, Phys. Reports, in press

Bonazzola S., Gourgoulhon E., Salgado M., Marck J.A., 1993, A&A 278, 421

Bonazzola S., Frieben J., Gourgoulhon E., 1995, ApJ, 460, 379

Brown G.E., Bethe H.A., 1994, ApJ 423, 659

Burrows A., Lattimer J.M., 1986, ApJ, 307, 178

Cook G.B., Shapiro S.L., Teukolsky S.A., 1994, ApJ 424, 823

Cutler C., Lindblom L., Splinter R.J., 1990, ApJ 363, 603

Friedman J.L., Ipser J.R., Sorkin R.D., 1988, ApJ 325, 722

Friedman J.L., Ipser J.R., Parker L., 1989, Phys. Rev. Lett. 62, 3015

Friedman J.L., Ipser J.R., 1992, Phil. Trans. R. Soc. Lond. A, 340, 391

Haensel P., Zdunik J.L., 1989, Nature 340, 617

Haensel P., Salgado M., Bonazzola S., 1995, A&A 296, 745

Hashimoto M-A, Oyamatsu K., Eriguchi Y., 1995, ApJ 436, 257

Ipser J.R., Lindblom L., 1991, ApJ 373, 213

Janka H.-T., Moenchmeyer R., 1989a, A&A, 209, L5

Janka H.-T., Moenchmeyer R., 1989b, A&A, 226, 69

Kazanas D., 1977, Nature 267, 501

Lai D., Shapiro S.L., 1995, ApJ, 442, 259

Lattimer J.M., Swesty F.D, 1991, Nucl. Phys. A535, 331

Lindblom L., 1995, ApJ 438, 265

Moenchmeyer R., Mueller E., 1989, in "Timing Neutron Stars", ed. Oegelman H., van den Heuvel E.P.J, Kluwer, Dordrecht

Nozawa T., Hashimoto M., Oyamatsu K., Eriguchi Y., 1996, Phys. Rev. D 53, 1845

Pandharipande V.R., Pethick C.J., Thorsson V., 1995, Phys.Rev.Lett. 75, 4567

Salgado M., Bonazzola S., Gourgoulhon E., Haensel P., 1994, A&A 291, 155

Sawyer R.F., 1980, ApJ 237, 187

Sawyer R.F., Soni A., 1979, ApJ 230, 859

Shapiro S.L., Teukolsky S.A., Wasserman I., 1989, Nature 340, 451

Sorkin R.D., 1982, ApJ 257, 847

Stergioulas N., Friedman J.L., 1995, ApJ 444, 306

Takatsuka T., 1995, Nucl. Phys. A588, 365

Tassoul J.L., 1978, "Theory of rotating stars", Princeton University Press, Princeton

Yoshida S., Eriguchi Y., 1995, ApJ 438, 830

Zdunik J.L., 1996, A&A 308, 828